fib WILEY

TECHNICAL PAPER

Critique of critical shear crack theory for *fib* Model Code articles on shear strength and size effect of reinforced concrete beams

Abdullah Dönmez[1,2] | Zdeněk P. Bažant[2]

[1]Istanbul Technical University, Department of Civil Engineering, Istanbul, Turkey

[2]Northwestern University, Department of Civil & Environmental Engineering, Evanston, Illinois

Correspondence

Zdeněk P. Bažant, Department of Civil & Environmental Engineering, Northwestern University, 2145 Sheridan Road, CEE/A135, Evanston, IL 60208.
Email: z-bazant@northwestern.edu

The size effect of Muttoni et al.'s critical shear crack theory (CSCT) is shown to be quite close (with differences up to 15%) and asymptotically identical to the energetic size effect law (SEL), which has been extensively verified experimentally and theoretically (and is adopted for the 2019 ACI Code, Standard 318, for both beam shear and punching). However, the CSCT derivation and calculation procedure obfuscates the mechanics of failure. It is shown to rest on six scientifically untenable hypotheses, which would have to be taught to students as an article of faith. They make CSCT untrustworthy outside the testing range; ditto for beams with T, I and box cross section, or for continuous beams. The present conclusions are supported by experimentally calibrated finite element simulations of crack path and width, of stress distributions and localizations during failure, and of strain energy release. The simulations also show the CSCT to be incompatible with the "strut-and-tie" model, which is (for 2019 ACI Code) modernized to include the size effect in the compression strut. Finally, further deficiencies are pointed out for the Modified Compression Field Theory (MCFT), currently embedded in the Model Code.

KEYWORDS

brittleness, concrete fracture, design codes, energy criteria, finite elements simulations, fracture mechanics, mechanics of concrete, scaling, shear failure, structural strength

1 | NATURE AND EVOLUTION OF SIZE EFFECT FORMULAE IN DESIGN CODES

Half a century ago, experiments in Stuttgart,[1–3] Toronto,[4,5] and Tokyo[6] established the existence of a strong size effect in shear failure of reinforced concrete (RC) beams. Weibull's[7] statistical power-law size effect was already well known at that time, but was also known to apply only to structures in which formation of a small crack (or fractured representative volume element of material) within any one of many possible places in the structure volume generates a dynamic crack propagation and causes immediate failure.

This is obviously not the case for shear failure of RC beams, which tolerate extensive cracking and a long stable crack growth before reaching the ultimate load.

Based on energy release arguments adapted to quasibrittle fracture mechanics, a new energetic size effect law (SEL), applicable to failures occurring after stable growth of a long crack, as typical of shear failure of RC beams, was formulated in 1984.[8] Immediately,[9] the SEL was proposed to ACI for shear design of RC beams (as well as of prestressed beams[10]). Subsequently it was shown to apply to many types of failure in all quasibrittle materials,[11,12] which do not follow classical fracture mechanics. Aside from concrete, they also include tough ceramics, fiber composites, rocks, stiff soils, sea ice, wood, stiff foams, bone, etc. The SEL captures the transition from a nearly ductile behavior in

small concrete structures to a nearly brittle behavior in large ones. The reason for this ductile-brittle transition of structural response is the material heterogeneity, which causes the fracture process zone (FPZ) to be long (cca 0.5 m in concrete vs. micrometers in metals), and non-negligible compared to the cross section size.

The size effect theory based on quasibrittle fracture mechanics had to wait three decades to win broad acceptance in the engineering community. This long delay was mainly caused by various controversies generated by competing explanations of size effect—for example, the fractal nature of crack surfaces or of microstructure of concrete, the role of boundary layer, and the effects of initial crack spacing, of crack width, or of material randomness of various kinds.

In the 1980s, a generally accepted theory of quasibrittle failures was lacking. The Japan Society of Civil Engineers (JSCE) and Commité Européen du Béton (CEB), apparently thinking that "better something than nothing," introduced into their design specifications purely empirical equations for the size effect on the ultimate shear force[13] and on the cracking shear force,[14] respectively. Meanwhile, the ACI committees, cognizant of the enormous staying power of code specifications adopted by democratic voting of large committees, and thinking cautiously that "better nothing than something controversial," spent three decades in lively polemics until eventually deciding to adopt the SEL for the beam shear, slab punching and strut-and-tie specifications (which have been adopted for the 2019 version of ACI code, Standard 318).

Meanwhile, *fib* (fédération internationale du béton), the successor to CEB, made a change in its Model Code 2010.[15] It adopted the size effect equations based on the so-called "Modified Compression Field Theory" (MCFT) for beam shear and critical shear crack theory (CSCT) for punching shear.[15–19] The MCFT uses elementary, supposedly logical, arguments, in which the critical crack width, w, and a certain strain, ϵ, estimated from the classical elastic theory of beam bending, are imagined to be the failure indicators. Model Code 2010[15] specifies in its Equations (7.3-19) and (7.3-21) two approximations for beam shear capacity without stirrups—Level I and Level II. This paper will focus on Level II approximation. Level I, which is treated (according to equation (7.3-21) in Ref.15) as an approximation to Level II, will be only briefly examined in the Appendix.

Currently, the so-called CSCT,[18–20] extending a concept advanced in 1991,[21] is being proposed as an improvement of Model Code 2010 for beam (or one-way) shear. The Swiss Code[22] has already adopted the CSCT for both the beam shear and punching (two-way) shear, while Model Code 2010 has done so for the latter. The objective of this article is to call attention to the errors in CSCT.

2 | HYPOTHESES UNDERLYING THE CSCT THEORY

Careful examination shows that six hypotheses are implicit to CSCT. The average (or nominal) shear strength (or ultimate stress) in the cross section is denoted as $v_u = V_R/bd$ where V_R is the resistant shear force provided by concrete; d = depth of the cross section from the compressed face to the centroid of reinforcement; b = width.

Hypothesis 1 The shear force, V_R, carried by concrete at maximum load is (in CSCT as well as MCFT) assumed to be controlled by a characteristic crack width w of the dominant crack leading to failure.

Hypothesis 2 To express the size effect, it is assumed that (Equation (1) in Ref.19):

$$\frac{v_u}{\sqrt{f_c}} = \frac{\alpha_1}{1 + \alpha_2\left(w/d_{dg}\right)}, \alpha_1 = 1/3 \,(\text{in MPa, mm}) \qquad (1)$$

where α_2 is an empirical calibration constant; f_c is the mean compressive strength of concrete (both f_c and $\sqrt{f_c}$ is considered to be in MPa); and d_{dg} is called the equivalent surface roughness, calculated as $d_{dg} = \min(d_g + 16, 40 \text{ mm})$ where d_g refers the maximum aggregate size.

Hypothesis 3 The width of the dominant diagonal crack is assumed to be proportional to the reference strain, ϵ, that is,

$$w = \alpha_3 \epsilon d, \quad \alpha_3 = 120/\alpha_2 \qquad (2)$$

where α_3 is an empirical coefficient depending on α_2, and ϵ is an assumed reference strain, defined as the normal strain in the longitudinal direction, x, at a certain characteristic location, crossing the dominant crack (see the on-line equation above Equation (1) in Ref.19).

It may be noted that Hypotheses (1—3) could be merged from the viewpoint of practical application. But here they are better kept separate to clarify what are all the hypotheses implied in the derivation of CSCT, and allow their separate discussion in what follows.

Hypothesis 4 The reference strain, ϵ, is assumed to be the longitudinal normal strain at distance $d/2$ from the concentrated load $P = V_R$ toward the support, and at depth $0.6d$ from the top face of beam (Equation (2) in Ref. 19).

Hypothesis 5 The reference strain, ϵ, assumed to control crack width, is calculated according to the

linear elastic beam theory based on Bernoulli-Navier hypothesis of plane cross sections remaining plane (Equations (2) and (3) in Ref. 19), that is,

$$\epsilon = \frac{M}{bd\rho E_s(d-c/3)} \frac{\alpha_4 d - c}{d - c},$$
$$M = V_R(a - \alpha_5 d), \quad \alpha_4 = 0.6, \quad \alpha_5 = 1/2 \qquad (3)$$

and, according to the no-tension hypothesis of elastic flexure of concrete beams with one-sided reinforcement (Ref. 19 Equation (4)),

$$c = \alpha_6 d, \alpha_6 = \frac{\rho E_s}{E_c}\left(\sqrt{1 + \frac{2E_c}{\rho E_s}} - 1\right) \qquad (4)$$

where E_c, E_s = elastic moduli of concrete and of steel reinforcement, ρ = reinforcement ratio, c = distance of the neutral axis from the top face of beam (or the length of the triangular profile of elastic compression stress), a = shear span = distance between the concentrated load and the closest end support.

Hypothesis 6 The foregoing equations, based on linear elastic beam bending theory, are assumed to be applicable at maximum (or ultimate) load of beam, that is, at incipient shear failure under controlled load.

The foregoing notations could be simplified by replacing $\alpha_1 \ldots \alpha_5$ with numbers. But the general notations for the coefficients are here preferred because the values of these coefficients may change if the CSCT is recalibrated on a larger database (e.g., the ACI-445 database).

3 | BEAM SHEAR STRENGTH ACCORDING TO CSCT ENSUING FROM THE HYPOTHESES, AND COMPARISON WITH ACI-446

In dimensionless form, ϵ in Equation (2) (Hypotheses 3, 5, 6) can be written as.

$$\epsilon = \gamma v_u, \gamma = \frac{a - \alpha_5 d}{\rho E_s(d-c/3)} \frac{\alpha_4 d - c}{d - c} \qquad (5)$$

Substituting ϵ from Equation (2) into Equation (1) (Hypotheses 1, 2), one gets a quadratic equation for v_u. Solving it gives:

$$\frac{v_u}{\sqrt{f_c}} = \frac{-1 + \sqrt{1 + 4\alpha_1 C_1 d}}{2C_1 d}, C_1 = \frac{\alpha_2\alpha_3\gamma\sqrt{f_c}}{d_{dg}} \qquad (6)$$

which coincides with Equation (5) in Ref. 19. Multiplying both the numerator and denominator of the right-hand side of this equation with $1 + \sqrt{1 + 4\alpha_1 C_1 d}$, a more instructive form of this equation follows:

$$\frac{v_u}{\sqrt{f_c}} = \frac{2\alpha_1}{1 + \sqrt{1 + d/d_0^M}}, d_0^M = \frac{1}{4\alpha_1 C_1} \qquad (7)$$

This equation is in a form readily comparable to the size effect factor λ proposed by ACI Committee 445, Fracture Mechanics. This factor has been adopted for the 2019 version of ACI code (ACI Standard 318), and reads:

$$v_u = v_0\lambda, \lambda = \frac{1}{\sqrt{1 + d/d_0}} \qquad (8)$$

where d_0 is a constant, called the transitional size (in ACI taken as 10 in.).

It needs to be pointed out that ACI also includes a horizontal cutoff at $v_u = 2\sqrt{f_c'}$ (introduced by ACI-318E), which is not considered here because it is justified by statistics rather than mechanics, that is, by an increasing width of the database scatter band on approach to smaller d, which causes the lower bound of the scatter band at small sizes to be statistically almost independent of d.

An important feature is the asymptotics, which has been solidly established by quasibrittle fracture mechanics and is as follows:

$$\text{For } d/d_0 \rightarrow 0 : v_u = \text{constant};$$
$$\text{For } d/d_0 \rightarrow \infty : v_u \rightarrow (d/d_0)^{-1/2} \qquad (9)$$

These asymptotic properties are satisfied by both formulations. However, for the same transitional size, that is, for $d_0^M = d_0$, the size effect curves of $\log(v_u)$ versus $\log(d/d_0)$ differ significantly and the large-size asymptotes do not coincide; see Figure 1a.

Varying the ratio $k = d_0^M/d_0$ stretches the size effect curve horizontally but does not change the asymptotic slope of $-1/2$ in the log–log plot. Can the large size asymptotes be made to coincide by varying the k? To answer it, denote $q = d/d_0$, consider that the small-size asymptotes are matched, which occurs for $\alpha_1\sqrt{f_c} = v_0$, and seek the value of k for which the large size limit of the ratio of the size effect expressions in Equations (7) and (8) equals 1, that is,

$$\lim_{d \to \infty} \frac{v_u^M}{v_u} = \lim_{d \to \infty} \frac{2\sqrt{1+q}}{1 + \sqrt{1 + q/k}} = 1 \qquad (10)$$

The limit is $2\sqrt{k}$ and, equating it to 1, one finds that both the small-size asymptotic value, $\alpha_1\sqrt{f_c} = v_0$, and the large-size asymptotic condition in Equation (10) get matched if (Figure 1b):

$$k = 1/4 \quad \text{or} \quad d_0^M = d_0/4. \qquad (11)$$

Figure 1b shows that the difference, Δv_u, between the two curves asymptotically matched curves becomes 12.6% at $d = d_0$, which is not too large, though not insignificant for design.
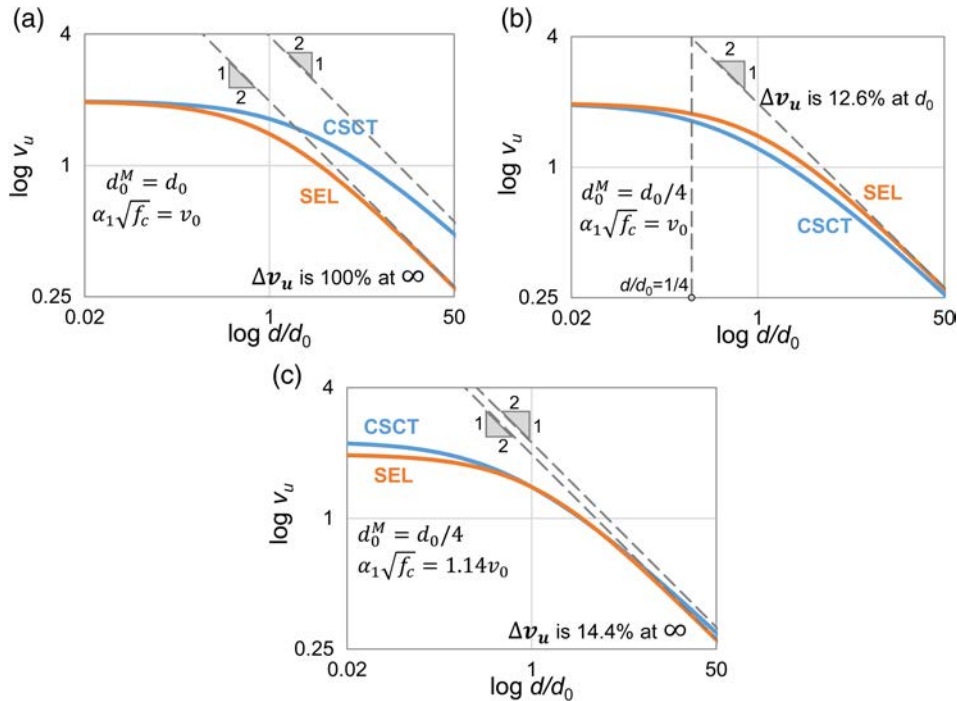
FIGURE 1 Size effect comparisons of SEL and CSCT for beam shear

Figure 1c further shows that if the curves are matched at $d_0 = d$, then the difference, Δv_u, between the two prediction curves becomes 14.4% at both the small-size and large-size asymptotes. Again, this is not too large, though not insignificant for design.

It may also be noted that Equations (1) with (2) was previously used in MCFT[16,23] without the dependence of w on ϵ, and was in this form adopted for the Level I Approximation in Model Code 2010. In that case, the size effect curve ended with asymptotic slope −1 instead of −1/2, which is thermodynamically impossible. The change to −1/2 was achieved by Muttoni and Fernández Ruiz's[18] artificial modification that added the fictitious dependence on ϵ and thus made w proportional to v_u. This then led to the quadratic equation for v_u, Equation (5), and thus changed the asymptotic slope from the (thermodynamically impossible) value −1 to the value −1/2 dictated by fracture mechanics.

4 | DEFICIENCIES OF CSCT REVEALED BY FE SIMULATIONS OF BEAM SHEAR FAILURE

Certain key aspects of failure, such as finding where the energy needed for fracture is coming from and where it is dissipated, are virtually impossible to observe in experiments directly. However, they can be revealed by extending experimental results with a realistic computer model. Microplane constitutive model M7[24,25] for softening damage in concrete, combined in finite element (FE) element analysis with the crack band model,[26,27] is such a model, as proven in many

previous studies (Refs. 28–30, e.g.) and also verified in Appendix 2 (which gives more information on the FE analysis). We will pursue the FE approach now, examining not only the energy flow but also other features important to understand the shear strength, such as the stress distributions across damage zones and along cohesive cracks, stress redistributions due to fracture and the overall response of structures of different sizes and shapes.

For the size effect analysis to make sense, the modes of failure, and particularly the shapes of dominant cracks in geometrically similar beams of different sizes, must also be geometrically similar. This fact has been experimentally best documented by the tests of Syroka-Korol and Tejchman,[31] as shown in figure 7 of Ref. 32.

Shear tests of geometrically similar RC beams of different sizes, without stirrups, have been simulated with FE program ABAQUS. The microplane damage constitutive model M7 has been implemented in user's subroutine VUMAT. The carefully conducted experiments of beam shear failure performed in M. Collins' lab at the University of Toronto[23] are chosen to calibrate the FE element code with constitutive model M7, as detailed in Appendix 2.

Figure 2a shows, in relative coordinates scaled with the beam size, the FE meshes for nearly similar beams of two sizes, which are $d = 110$ mm and 924 mm (this gives the size ratio 8.41:1). The FE size is the same for all beam sizes, so as to avoid dealing with spurious mesh size sensitivity. The blackened elements in Figure 2 show, for maximum load P_{max}, the locations of the highest longitudinal strains in the element. Note that the band of blackened elements runs faithfully along the upper side of main crack (the width of
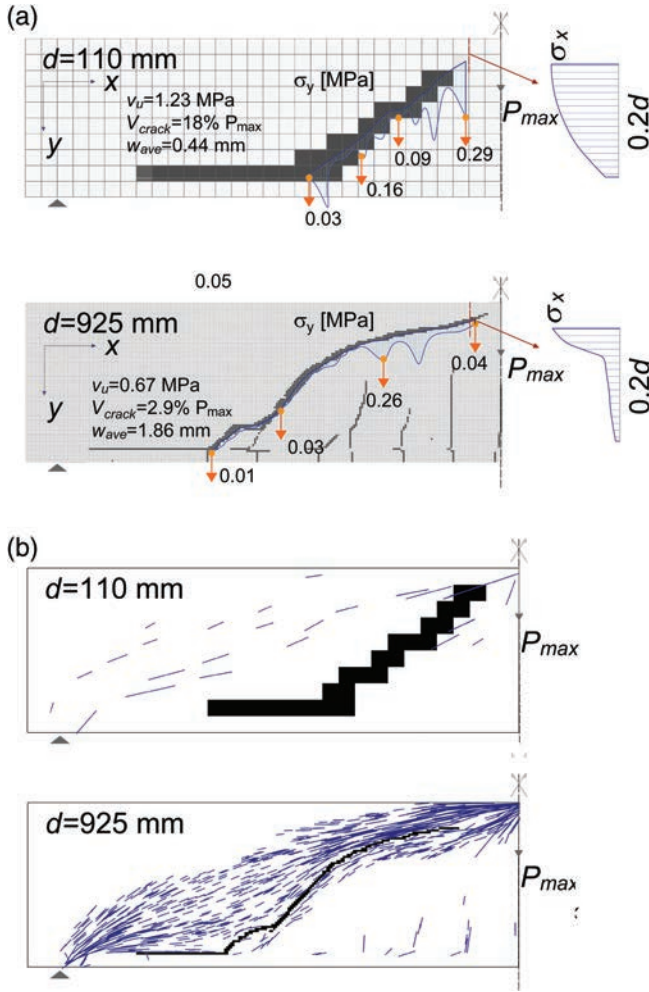
FIGURE 2 (a) Longitudinal stress variation across ligament above the main crack tip (on the right of beam) and variation of vertical stress component along the diagonal crack, (b) the vectors of minimum principal compressive stresses (maximum in magnitude) calculated for Toronto test beams[23]

the blackened band is the finite element width and has nothing to do with the crack width).

4.1 | Localizing stress distributions

Figure 2a shows, to the right of the beams, the distributions of longitudinal normal stress σ_x across the height of the ligament (understood as the zone between the tip of the dominant diagonal shear crack at P_{max} and the top face). These distributions (which are similar to those in Ref. 33 and in figure 11 of Ref.32) demonstrate how the stresses localize near the top face as the size d is increased. It is evident that, in the smallest beam, the material strength across the ligament is utilized almost in full (for plastic behavior it would be mobilized fully). In the largest beam, by contrast, the material strength is, at P_{max}, localized within only a small portion of the ligament. This localization provides an intuitive explanation of the size effect (see also Refs.33–35). What do these distributions have in common with the crack opening at depth $0.6d$, and generally with Hypotheses (3) and (5)? Nothing.

4.2 | Cross-crack stress transmission

Figure 2a reveals, for beams of two sizes, another relevant feature impossible to measure directly—the distribution of the vertical stress component transmitted, at P_{max}, across the crack. The numbers at the vertical arrows represent, as a percentage of tensile strength of concrete, the vertical stress transmitted at P_{max} across the diagonal shear crack due to the aggregate interlock or cohesive softening. Here it is important to notice that, except near the crack tip, the percentages are quite low, and that they decrease markedly with the beam size.

Especially note in Figure 2a the vertical forces V_{crack} indicated as percentages of the total shear force, $V_c = P_{max}$, obtained by integrating the vertical cross-crack stress components along the whole crack length. They represent for the beams of small and large sizes, respectively, only 18 and 2.9% of the total shear force V_c. If the vertical force transmitted at P_{max} across the crack is so small, how could the crack width, w, play any significant role? It could not. Therefore, Hypotheses (2–5) are unjustified, unrealistic.

Figure 2b shows the vectors of minimum principal compressive stresses (maximum in magnitude). They confirm that the load just before the failure (i.e., at P_{max}) is transmitted mainly by a strip of concrete along the top side of the crack. In the sense of the strut-and-tie model, this strip represents what is called the "compression strut." The fact that these vectors generally do not cross the crack means that the force transmitted across the crack at P_{max} is negligible. This again contradicts Hypotheses (2)–(5).

4.3 | Scenario of energy release and dissipation

Most relevant for fracture is the energy picture, shown in Figure 3. Fracture dissipates energy, and that energy must come from somewhere. At controlled displacement, it must come solely from the release of potential energy (i.e., strain energy) from the structure. As proposed by Griffith in 1921,[11] this release is a central tenet of fracture mechanics of all types, including quasibrittle fracture. So we calculate, for all the integration points of all the elements, the density of strain energy released at unloading:

$$\Pi = \frac{1}{2}\sigma^T C\sigma \qquad (12)$$

which is an important quantity that cannot be directly measured; C is the 6×6 matrix of elastic compliances for unloading (i.e., inverse of the elastic moduli matrix), and σ is the 6×1 column matrix of stress components, as affected by distributed fracturing (for simplicity, the unloading stiffness is considered the same as the initial elastic stiffness). Then, considering all the integration points, we calculate the change of energy density in each integration point between these two states; in this case

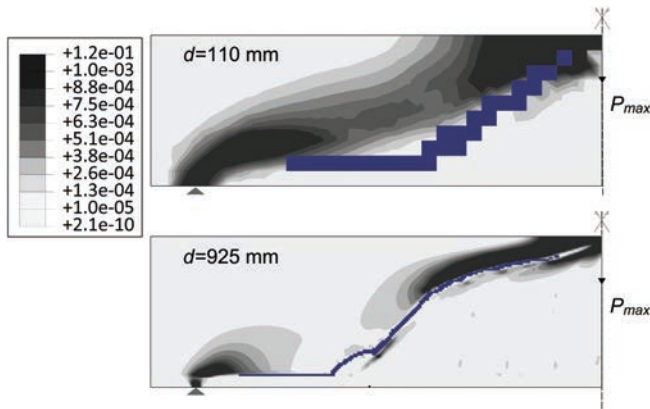$$\Delta\Pi = \Pi_{99} - \Pi_0 \qquad (13)$$

FIGURE 3 Energy release zones in relative coordinates, calculated for Toronto test beams[23]

which is the change from the value Π_{99} for the prepeak state at load $P = 0.99P_{max}$, to the value Π_0 for the postpeak state at which the load has been reduced to 0 (other states could be chosen, too; but for states close to each other the changes would have high numerical scatter).

The energy density difference $\Delta\Pi$ represents the values of energy density release at each integration point of the finite elements. From all these values, one can compute the contour plots of the zones of energy release density. These zones are shown in relative coordinates in Figure 3, where the zone of maximum density is shown as dark. Note that, in actual coordinates, the dark band for the largest beam would be much wider than for the smallest beam.

The dark band of the energy release may be imagined to represent the "compression strut" of strut-and-tie model. The strut is located wholly above the main crack. On top of the strut, the energy release comes from damaging concrete, and in the rest of strut from the unloading of undamaged concrete. The main diagonal shear crack does not contribute to the dominant energy changes, especially not for large beams. So how can it play a significant role in controlling the failure load? Again this contradicts Hypotheses (3) and (5).

The essential idea of the SEL is that the total energy release from the structure is a sum of two parts, $\bar{\Pi} = \bar{\Pi}_1 + \bar{\Pi}_2$, where $\bar{\Pi}_2$ is the total strain energy released by unloading from the undamaged part of the structures whose volume increases (for geometric scaling) *quadratically* with the structures size (d in our case), and $\bar{\Pi}_1$ is the total strain energy released by unloading from the damaged part (traveled through by the FPZ) whose volume increases *linearly* with the structure size, whereas W, the energy dissipated (which must be equal to $\bar{\Pi}$) increases always *linearly* with structure size. The ratio of the quadratic to linear increases immediately indicates that, for small enough sizes, the quadratic part, $\bar{\Pi}_2$, must be *negligible* compared to the linear part, $\bar{\Pi}_1$, while for large enough sizes it must be *dominant*.

In our problem, further evaluation of the FE results could show that the total energy dissipation by fracturing damage increases roughly *linearly* with the shear crack length, which

is proportional to beam size d, while the energy released from the undamaged part of the dark band (or compression strut) on the side of the main crack increases roughly *quadratically* with d because not only the length but also the width of the dark band (or the strut) in Figure 3 increases roughly in proportion to d. Thus the mismatch of linear and quadratic increase is the ultimate source of transition in the size effect curve for beam shear.

The aforementioned energy derivation of the SEL, is, in fact, much simpler than that of CSCT (see Appendix 3, and also the 1984 study[8] in which the SEL was first formulated). Energy conservation and dimensional analysis is the essence of a fundamental but simple derivation of the SEL as given in Equations (5)–(7) of Ref. 32 and summarized in Appendix 3.

4.4 | Compatibility with modernized strut-and-tie model

The strut-and-tie model (originally called Mörsch's truss analogy, 1903) is generally considered to provide good estimates of limit loads of concrete structures. In the classical form, however, the strut-and-tie model misses the size effect. In Ref. 36 it was shown how the strut-and-tie model could be modernized by calculating the balance of energy dissipated by compression-shear crushing on top of the compression strut, with the energy release from the intact and damaging parts of the compression strut.

Recently it has become widely accepted that the strut-and-tie model must be modernized by incorporating the size effect into the compression struts (and this has actually been adopted for ACI Standard 318-2019). In view of the foregoing observations about the energy release zone and the energy dissipation zone on top of the strut, such a modernization is simple, obvious and logical—simply introduce the size effect into the compression strut.

The concept of a modernized "compression strut" exhibiting a size effect is in concert with the SEL, agrees with the present analysis (Figure 4) as well as with the conclusions in Refs. 33, 36. Does not this agreement invalidate the hypotheses of CSCT? It certainly does. It must be concluded that the CSCT approach is incompatible with the modernized strut-and-tie model, whereas the SEL is.

5 | UNFOUNDED AND SCIENTIFICALLY DUBIOUS ASPECTS OF THE HYPOTHESES

Re Hypothesis 1. According to the FE simulations, the crack width w is highly variable along the crack length. Which opening, w, and at which location and beam size, would produce the
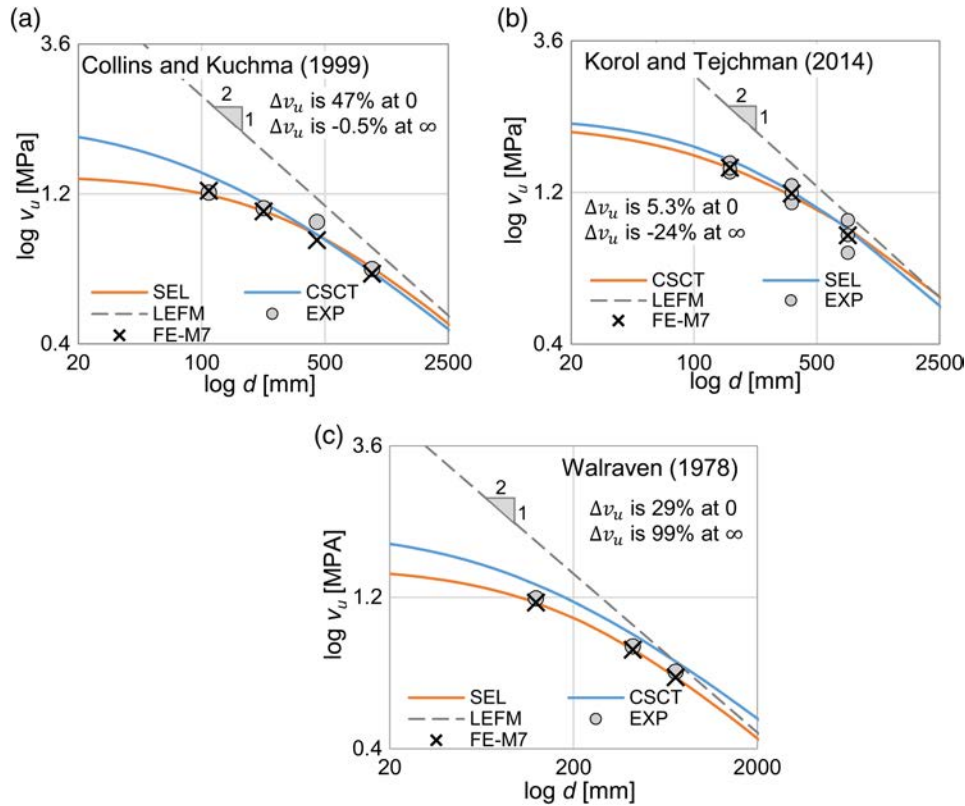
FIGURE 4 Comparison of test data: (a) from Ref. 23, (b) from Ref. 31, and (c) from Ref. 43 with finite element (FE) results and the size effect curves of SEL (Equation (8)) and critical shear crack theory (CSCT) (Equation (1)) (Δvu are the percentage errors of CSCT compared to SEL fits)

cohesive stress that matters for the ultimate shear force v_u? There is no answer.

Re Hypothesis 2. A basic concept of the cohesive crack model, which includes cohesion due to the aggregate interlock, is the decrease of crack-bridging cohesive stress σ_c with increasing crack opening width w. This is a property studied for concrete in great detail since 1980.[37] Already by 1990 it became clear that Equation (1), with w appearing linearly in the denominator, agrees neither with the experimental evidence on postpeak softening of cracks in concrete, nor with FE simulations. It is now generally accepted that the cohesive softening curve is approximately bilinear, with a steep initial drop followed by a very long tail (Refs. 38, 39 e.g.).

If the denominator of Equation (1) were anything but linear in w, substitution of Equation (2) into Equation (1) would not yield for CSCT a quadratic equation for w (Equation (5) in Ref.18), and then the large size asymptote of size effect would not have slope $-1/2$ in log-scale. So the motivation for Equation (1) seems to be to manipulate the derivation so as to obtain an

asymptote of slope $-1/2$, which is by now a widely accepted fact.

Re Hypothesis 3. Why should the crack width, and thus the ultimate load and the size effect, be determined by the product of beam depth d with strain ϵ at some specific location? That is a fiction, and is impossible in fracture mechanics.

Can one identify in the present FE results any characteristic strain controlling the ultimate load? Certainly not. What matters for fracture is the release of stored strain energy from the structure and, in the case of cohesive (or quasibrittle) fracture, also the tensile strength of material. Certainly not any particular strain.

Re Hypothesis 4. This is a mystery. Why should the reference strain, ϵ, be taken at distance $d/2$ from the concentrated load, and why at depth $0.6d$ from the top face? These values are empirical, resulting from an effort to match some of the experimental evidence. Besides, these values would surely have to change in the case of continuous beams and T, I, or box cross sections, for which the moment-curvature relations are different.

Re Hypothesis 5. Why should the reference strain, ϵ, be calculated according to linear elasticity if, at ultimate load, the concrete behaves highly nonlinearly, due to cracking damage? This is a fiction.

And why, in the first place, should the strain be chosen as an indicator of size effect? As is well known, in elastic or elasto-plastic geometrically similar structures, the strain at homologous points is the same for all structure sizes. To overcome this inconvenient fact is what leads to the mystic Hypothesis (3) (Equation (2)).

And why should the strain analysis use the classical beam bending theory based on the Bernoulli-Navier hypothesis, which applies only in the flexure of sufficiently slender beams? Fiction again.

The FE analysis shows the initially plane cross sections at ultimate load to be highly warped. Formulas to calculate ϵ based on inelastic behavior would, of course, be awfully complicated. But why to bother with calculating this strain at all? It is not the cause of failure. The real cause of quasibrittle failures and size effect is the overall energy release from the structure.

Re Hypothesis 6. The overall spirit of the size effect calculation in CSCT (as well as MCFT) is to avoid fracture mechanics and replace it by some sort of simple linear elastic beam analysis. But this analysis is just an artifice, aimed to provide a semblance of logic.

6 | CAN CSCT BE EXTENDED TO DESIGNS OUTSIDE THE RANGE OF EXISTING TESTS?

The bulk of the existing tests of size effect in beam shear strength involved a relatively limited range of geometries, in terms of shear-span ratio and reinforcement types, and did not include continuous beams. It is questionable whether the CSCT, beginning with the elastic strain at $0.6d$ depth, and at distance $d/2$ from the concentrated load, could be applied to such situations. It is also questionable, as pointed out earlier, to apply the CSCT to other cross section geometries.

On the other hand, the size effect factor λ, Equation (8) based on SEL, is, in principle, applicable to all quasibrittle failures (geometrically similar for different sizes), in which a long stable crack develops prior to reaching the maximum load and an unlimited postpeak plastic plateau is lacking (see also Appendix 3). Generally, it suffices to multiply with λ the limit analysis formula for the strength contribution of concrete that works for small beam sizes. The only parameter that needs to be estimated is the transitional size d_0, although one can assume that it varies negligibly within the normal range of geometries.

7 | SHOULD NOT THE DESIGN CODE HEED THE IDEALS OF SIMPLICITY AND GENERALITY?

The main problem with Equation (6) or (7) of CSCT is not that it would be unsafe to a large degree. It is not. The problem is that the fictitious derivation obfuscates the mechanics of failure and is much more complicated than necessary to obtain a realistic size effect prediction. Just compare the derivation discussed above with the general derivation of SEL in Equations 4–7 in Ref. 32, based solely on the energy conservation and dimensional analysis (as summarized in Appendix 3), or to the original 1984 derivation in Ref. 8, based on approximation of energy release in presence of a localization limiter, the characteristic size of the FPZ.

These, as well as several other, derivations of the SEL are much simpler, and are based on only three hypotheses—the relevance of energy release, geometrical similarity of the dominant large crack in structures of different sizes, and the approximate size independence of the FPZ (which represents a characteristic length, as a material property). These hypotheses are obvious, generally accepted, and generally applicable to many types of structures and materials. These are all the quasibrittle materials which, aside from concrete and mortar, also include the fiber-polymer composites, tough ceramics, sea ice, many rocks, stiff soils, masonry, wood, etc. They all exhibit the same kind of size effect on nominal structural strength.

So why should the size effect in concrete be different? Concrete shear failure is not as exceptional as the derivation of CSCT suggests. Rather it is just one manifestation of a typical size effect exhibited by many materials and structures. So why should the beam shear need a special derivation, not applicable to all the other similar situations? Is it not strange that the purported derivation underlying the size effect of the CSCT (or the MCFT and Model Code 2010) cannot be transplanted to other quasibrittle materials? Why should concrete, and the shear of beams, be so *unique*?

Besides, a formulation based on the energy release concept of fracture mechanics (based on the work of Ballarini at Northwestern in the 1980s) has already been used for a long time in most design codes, to predict the shear failure in the pullout of anchors from concrete walls, including the size effect. How come that, for one type of shear failure of concrete, the fracture mechanics basis of size effect is accepted in the Model Code, while for another type of shear failure it is not?

8 | COMMENTS ON THE ANALOGOUS PROBLEM OF SIZE EFFECT ON PUNCHING SHEAR STRENGTH OF SLABS

As demonstrated in Refs. 28, 40 the punching shear strength of slabs also follows the SEL derived from energy release (and the SEL size effect factor is also adopted for the 2019 version of the ACI Standard 318). Nevertheless, an alternative

size effect calculation based on CSCT, resting on elementary mechanics of bending, was incorporated into Model Code 2010. Muttoni et al.[41] adapted their CSCT to punching with the modification that a certain reference slab rotation is used instead of the reference strain. For punching they thus obtain a size effect that ends with the asymptotic slope of −0.4 (instead of −0.5), which is not correct but at least does not violate the second law of thermodynamics. The hypotheses in the derivation are again unjustified and fictitious.

9 | CONCLUSIONS

1. The shear size effect of the CSCT exhibits the correct small-size and large-size asymptotic behaviors, and appears to fit the size effect test data almost as well as the energetic SEL. Compared to SEL, the CSCT gives strength differences up to 14%, which are not large, though not insignificant for design. For CSCT, a nonlinear size effect regression of a large database, such as that of ACI-445 in Ref. 35, is lacking. The previous comparisons of SEL to many individual tests of diverse geometries included in that database have not been replicated for the CSCT.

2. The size effect of CSCT is based on a simplistic derivation devised to give a semblance of logical support in mechanics. The method of calculation of CSCT (as well as MCFT) is misleading. It is a "cook-book" procedure that has no logic and obfuscates the mechanics of shear failure. It would have to be taught to students as an article of faith.

3. The CSCT is shown to rest on six implied hypotheses. They are all physically unjustified. They involve application of the classical one-dimensional elastic beam bending theory to what is a multidimensional nonlinear problem of fracture mechanics. The same can be said about the hypotheses implied by the MCFT and Model Code 2010.

4. Finite element simulations with the M7 constitutive model, calibrated and verified here by the classical Toronto tests, extend the measured data by showing that, within the ligament between the tip of the main crack and the beam top, the stress profile is nearly uniform for small beams and rather localized for large beams. This means that, at maximum load, the concrete strength gets mobilized, for small beams, over almost the full length of the ligament while, for large beams, within only short portion of the length.

5. According to finite element results, the energy dissipation during fracture comes mainly from a highly stressed band on the side of the main shear crack and from a small damage zone above the tip of that crack. The main shear crack dissipates during failure almost no energy and thus, contrary to CSCT, its opening width cannot be what controls failure. This observation suffices to invalidate the CSCT (as well as MCFT).

6. Because of the lack of support in mechanics, the CSCT cannot be trusted for extensions to designs outside the range of the bulk of the existing size effect test data, which include different reinforcement types and shear spans, different cross sections, different distributions of shear force and bending moment as in continuous beams, etc.

7. The CSCT, as well as MCFT, is incompatible with the strut-and-tie model, while the SEL is, provided that the size effect is incorporated into the compression strut (which is already adopted for ACI Standard 318-2019).

8. The size effect of MCFT, incorporated into Model Code 2010, shows major deviations from the SEL. It has an incorrect large-size asymptote that is thermodynamically inadmissible and, consequently, it mispredicts the size effect in large beams.

NOTATIONS

a	shear span
a_c	the length of the fracture or crack band at maximum load
b	characteristic width of the beam cross section
b_w	width of beam
c	compression zone thickness of beam
$\mathbf{C}$	6×6 matrix of elastic compliances for unloading (i.e., inverse of the elastic moduli matrix)
C_1	variable defined in Equation (6)
$c_1, c_2,$ c_3, c_4	variables equal to 520, $1500c_5\sqrt{f_c}$, 1,000 and d_{dg} respectively
c_5	variable defined in Equation (A3)
d	depth of the cross section from the compressed face to the centroid of reinforcement
d_g	maximum aggregate size
d_{dg}	equivalent surface roughness and equals to min $(d_g + 16, 40 \text{ mm})$
d_0	transitional size which equals to materials' characteristic lengths times structure shape parameters
d_0^M	transitional size equivalence in the CSCT's equation
E	Young modulus
E_c, E_s	elastic moduli of concrete and of steel reinforcement
F	variable defined in Equations (A4) and (A5)
f_1, f_2	derivatives with respect to β_1 and β_2 used in Equation (C3)
f_c	mean compression strength of concrete
G_f	critical value of energy release rate
k	variable defined as $k = d_0^M / d_0$
k_v	the ultimate shear force normalized by $f_c^{0.5}$
M	bending moment
P_{max}	the maximum load

q	variable defined as $q = d/d_0$
V_c	total shear force
V_{crack}	the vertical forces transferred by the crack.
v_0	average shear strength of concrete for vanishing size d
V_R	resistant shear force provided by concrete
v_u	average shear strength
v_u^M	average shear strength of concrete in MC2010
w	crack width
W	the energy dissipated (which must be equal to Π)
w_c	a material constant equals to the width of crack band swept by FPZ
z	effective shear depth of beam according to the MC2010
$\alpha_1 \dots \alpha_5$	coefficients which follows $\alpha_1 = 1/3$, $\alpha_2\alpha_3 = 120$, $\alpha_4 = 0.6$, $\alpha_5 = 0.5$
β_1, β_2	variables defined as $\beta_1 = a_c/d$ and $\beta_2 = w_c a_c/d^2$, see Equation (C1)
$\Delta\Pi$	change of energy density
ϵ	longitudinal reference strain located below $0.6d$ of the compression face and $d/2$ distance of the applied load
γ	variable defined in Equation (5)
λ	size effect factor of SEL
Π	density of strain energy released at unloading
Π_{99}	strain energy density for prepeak state at load $P = 0.99 P_{max}$
Π_0	strain energy density for postpeak state at zero load
$\bar{\Pi}_1$	strain energy released by unloading from the damaged part of the structures
$\bar{\Pi}_2$	strain energy released by unloading from the undamaged part of the structures
ρ	longitudinal reinforcement ratio
σ	6×1 column matrix of stress components
σ_c	crack-bridging cohesive stress
σ_x	longitudinal normal stress across the height of the ligament

ORCID

Zdeněk P. Bažant https://orcid.org/0000-0003-0319-1300

REFERENCES

1. Leonhardt F, Walter R. Beiträge zur Behandlung der Schubprobleme in Stahlbetonbau. Beton und Stahlbetonbau. 1962;57(3):54–64.
2. Leonhardt, F., Walter, R., & Dilger, W. (1964). Shear Tests on Continuous Beams. Deutscher Ausschuss für Stahlbeton. No. 163, 138.
3. Bhal, N. S. (1968). Uber den Einfluss der Balkenhöhe auf Schubtragfähigkeit von einfeldrigen Stalbetonbalken mit und ohne Schubbewehrung. (Dissertation, Univ.). Stuttgart, Stuttgart, Germany.
4. Kani GNJ. Basic facts concerning shear failure. ACI J. 1966;63(6):675–692.
5. Kani GNJ. How safe are our large reinforced concrete beams. ACI J. 1967; 64(3):128–141.
6. Iguro, M., Shioiya, T., Nojiri, Y., & Akuyama, H. (1985). Experimental studies on shear strength of large reinforced concrete beams under uniformly distributed load. Concrete Library International, (Japan Soc. of Civil Engrs.). No. 5, p. 137–154 (transl. from JSCE 1984).
7. Weibull W. A statistical theory of the strength of materials. Proc R Swedish Acad Eng Sci. 1939;151:1–45.
8. Bažant ZP. Size effect in blunt fracture: Concrete, rock, metal. ASCE J Eng Mech. 1984;110(4):518–535.
9. Bažant ZP, Kim J-K. Size effect in shear failure of longitudinally reinforced beams. ACI J. 1984;81(5):456–468.
10. Bažant ZP, Cao Z. Size effect in shear failure of prestressed concrete beams. ACI J. 1986;83(2):260–268.
11. Bažant ZP, Planas J. Fracture and size effect in concrete and other Quasibrittle materials. Boca Raton and London: CRC Press, 1998.
12. Bažant, Z. P. (2002). Scaling of Structural Strength. Hermes Penton Science (Kogan Page Science), London; 2nd updated ed., Elsevier, London 2005 (Errata: www.civil.northwestern.edu/people/bazant.html) (French translation (with updates), Introduction aux effets d echelle sur la resistance des structures, Herm'es Science Publ., Paris 2004).
13. Subcommittee on English Version of Standard Specifications for Concrete Structures (2007). JSCE guidelines for concrete no. *15*: Design. Japan Society of Civil Engineering.
14. Fédération Internationale du Béton (*fib*): CEB *fib* Model Code 1990: Design Code, Comité Euro-International du Béton; nos.213/214.
15. Fédération Internationale du Béton (*fib*): Model Code 2010, final draft, vol. 1, Bulletin 65, and vol. 2, Bulletin 66, Lausanne, Switzerland, 2012.
16. Bentz EC, Vecchio FJ, Collins MP. Simplified modified compression field theory for calculating shear strength of reinforced concrete elements. ACI Mater J. 2006;103(4):614.
17. Sigrist V, Bentz E, Fernández Ruiz M, Foster S, Muttoni A. Background to the *fib* model code 2010 shear provisions. Part I: Beams and slabs. Struct Concr. 2013;14(3):195–203.
18. Muttoni A, Fernández Ruiz M. Shear strength of members without transverse reinforcement as function of critical shear crack width. ACI Struct J. 2008;105(2):163–172.
19. Fernández Ruiz M, Muttoni A. Size effect in shear and punching shear failures of concrete members without transverse reinforcement: Differences between statically determinate members and redundant structures. Struct Concr. 2018;19(1):65–75.
20. Fernández Ruiz M, Muttoni A, Sagaseta J. Shear strength of concrete members without transverse reinforcement: A mechanical approach to consistently account for size and strain effects. Eng Struct. 2015;99:360–372.
21. Muttoni, A., & Schwartz, J. (1991). Behavior of beams and punching in slabs without shear reinforcement. In: IABSE colloquium (Volume 62, No. CONF). IABSE Colloquium.
22. Swiss Society of Engineers and Architects, SIA Code 262 for Concrete Structures, Zürich, Switzerland, 2003, 94 pp.
23. Collins MP, Kuchma D. How safe are our large, lightly reinforced concrete beams, slabs, and footings? ACI Struct J. 1999;96(4):482–490.
24. Caner FC, Bažant ZP. Microplane model M7 for plain concrete: I. Formulation. ASCE J Eng Mech. 2013;139(12):1714–1723.
25. Caner FC, Bažant ZP. Microplane model M7 for plain concrete: II. Calibration and verification. ASCE J Eng Mech. 2013;139(12):1724–1735.
26. Bažant ZP, Oh BH. Crack band theory for fracture of concrete. Mater Struct (RILEM, Paris). 1983;16(3):155–177.
27. Červenka J, Bažant ZP, Wierer M. Equivalent localization element for crack band approach to mesh-sensitivity in microplane model. Int J Numer Methods Eng. 2005;62(5):700–726.
28. Dönmez A, Bažant ZP. Size effect on punching strength of reinforced concrete slabs with and without shear reinforcement. ACI Struct J. 2017;114(4):875–886.
29. Vorel J, Bažant ZP. Size effect in flexure of prestressed concrete beams failing by compression softening. ASCE J Struct Eng. 2014;140(10):04014068.
30. Rasoolinejad M, Bažant ZP. Size effect on strength of squat shear walls extrapolated by microplane model M7 from lab tests. ACI Struct J. 2018; in press (also SEGIM Report 18-10/788c, Northwestern University, Evanston).
31. Syroka-Korol E, Tejchman J. Experimental investigations of size effect in reinforced concrete beams failing by shear. Eng Struct. 2014;58:63–78.
32. Yu Q, Le J-L, Hubler HH, Wendner R, Cusatis G, Bažant ZP. Comparison of main models for size effect on shear strength of reinforced and prestressed concrete beams. Struct Concr (*fib*). 2016;17(5):778–789.
33. Bažant ZP, Yu Q. Designing against size effect on shear strength of reinforced concrete beams without stirrups: II. Verification and calibration. ASCE J Struct Eng. 2005;131(12):1885–1897.

34. Bažant ZP, Yu Q. Designing against size effect on shear strength of reinforced concrete beams without stirrups: I. Formulation. ASCE J Struct Eng. 2005;131(12):1877–1885.

35. Bažant ZP, Yu Q, Gerstle W, Hanson J, Ju JW. Justification of ACI 446 proposal for updating ACI code provisions for shear design of reinforced concrete beams. ACI Struct J. 2007;104(5):601–610.

36. Bažant ZP. Fracturing truss model: Size effect in shear failure of reinforced concrete. ASCE J Eng Mech. 1997;123(12):1276–1288.

37. Walraven, J. C., & Reinhardt, H. W. (1981). Concrete mechanics. Part A: Theory and experiments on the mechanical behavior of cracks in plain and reinforced concrete subjected to shear loading. NASA STI/Recon Technical Report N, 82.

38. Hoover CG, Bažant ZP. Cohesive crack, size effect, crack band and work-of-fracture models compared to comprehensive concrete fracture tests. Int J Fracture. 2014;187(1):133–143.

39. Hoover CG, Bažant ZP, Vorel J, Wendner R, Hubler MH. Comprehensive concrete fracture tests: Description and results. Eng Fract Mech. 2013;114:92–103.

40. Bažant ZP, Cao Z. Size effect in punching shear failure of slabs. ACI Struct J. 1987;84(1):44–53.

41. Muttoni A, Fernández Ruiz M, Bentz E, Foster S, Sigrist V. Background to fib Model Code 2010 shear provisions part II: Punching shear. Struct Concr. 2013;14(3):204–214.

42. Bentz EC, Collins MP. Development of the 2004 Canadian Standards Association (CSA) A23. 3 shear provisions for reinforced concrete. Can J Civ Eng. 2006;33(5):521–534.

43. Walraven, J. C. (1978). Influence of member depth on the shear strength of lightweight concrete beams without shear reinforcement. Stevin Report 5-78-4, Delft University of Technology.

AUTHORS' BIOGRAPHIES

A. Abdullah Dönmez, Postdoctoral Research Associate
Istanbul Technical University
Department of Civil Engineering
Istanbul, Turkey
Visiting Postdoc
Northwestern University
Evanston, Illinois
donmezab@itu.edu.tr

Zdeněk P. Bažant, McCormick Institute Professor, W.P. Murphy Professor Civil and Mechanical Engineering and Materials Science
Department of Civil & Environmental Engineering
Northwestern University
2145 Sheridan Road, CEE/A135,
Evanston, Illinois 60208
z-bazant@northwestern.edu

APPENDIX 1: DEFICIENCIES AND PROBLEMS OF MCFT AND OF MODEL CODE 2010

Although the MCFT, featured in the existing Model Code 2010, is not the focus of this study, some points are worth noting, for comparative purposes. The MCFT has more serious deficiencies than the CSCT. The Level I Approximation of Model Code 2010 consists of Equation (1) in which the value of w/d (and thus also ϵ) is not variable but is fixed. This gives $w\alpha_2 / d_{dg} = 1.25z$. Consequently, the large-size asymptotic behavior is.

$$\text{for } d \to \infty: \quad v_u \to \frac{\text{constant}}{d} \tag{A1}$$

Such asymptotic behavior is not supported experimentally. It is, in fact, thermodynamically impossible. Extrapolation to large sizes would severely exaggerate the size effect. At the same time, since the transition from the small-size (horizontal) to the large-size (inclined) asymptote is sharper and narrower than it is for the energetic size effect law (SEL), Equation (A1) underestimates the size effect in the mid-size range if the size effect is fitted to the same small-size data.

It may be noted that an equation of the same form as (A1) was proposed in Ref. 42 It found its way into the 2004 Canadian CSA A23.3 shear design provisions. A similar critique applies.

The Level II approximation of Model Code 2010 (or MCFT, Equation (4a) in Ref. 17) is written as

$$\frac{v_u}{\sqrt{f_c}} = k_v, \quad k_v = \frac{0.4}{1+1500\epsilon}\frac{1300}{1000+d_{dg}z} \tag{A2}$$

which may be rewritten as

$$k_v = \frac{c_1}{(1+c_2k_v)(c_3+c_4z)} \text{ with } c_2 = 1500c_5\sqrt{f_c}, \quad c_5 = \frac{a-d/2}{2d\rho E_s} \tag{A3}$$

in which $c_1 = 520$, $c_3 = 1{,}000$, $c_4 = d_{dg}$ are constants. Although this equation leads to a quadratic equation for k_v (different from Equation (1)), the asymptotic slope k_v for $z \to \infty$ may be more directly determined by replacing k_v with a new variable F such that

$$k_v = F/z \tag{A4}$$

Equation (A3) may then be rearranged as

$$F\left(1+c_2\frac{F}{z}\right)\left(\frac{c_3}{z}+c_4\right) = c_1 \tag{A5}$$

Now, assuming that F is a constant, the limit of this equation for $z \to \infty$ is $F(1+0)(0+c_4) = c_1$, that is, $Fc_4 = c_1$ or $F = c_1 / c_4$. This confirms our assumed constancy of F to have been correct and that $k_v = (c_1/c_4) / z$, or.

$$\text{for } z \to \infty : \ k_v = \frac{\text{constant}}{z} \tag{A6}$$

Such asymptotic behavior of Level II approximation of MCFT and of Model Code 2010 is, of course, also thermodynamically impossible, and thus untenable (same as for Level I). It also reveals a lack of scientific basis.

Most of the hypotheses of CSCT also apply to MCFT, and the previous criticisms need not be repeated.

APPENDIX 2: EXAMPLES VERIFYING REALISTIC PERFORMANCE OF MICROPLANE MODEL M7

The credibility of the foregoing FE analysis with model M7 depends on comparisons with experiments. Model M7 (whose coding can be freely downloaded from www.civil. northwestern.edu/people/bazant/), appears to be the only one that can match all types of material tests of concrete, as shown in Ref. 25. The M7, calibrated by a part of the data set on various structural tests, was shown to predict correctly the rest of the data set (Refs. 25, 28, 32, 33, e.g.). Here we show how well the M7 fits the strength and size effect of the three trusted experiments of beam shear failure and size effect[23,31,43] (similar demonstrations were also made in Refs. 32, 33).

Figure 4 shows the fitting of these tests,[23] used for calibration of M7. In Figure 4a, four-point-bend specimens of 4 different sizes (with only approximate geometric similarity) are simulated by finite elements (FE) using M7. The smallest and the largest effective depths are $d = 110$ mm and 925 mm. The flexural reinforcement ratio slightly varies from 0.76% to 0.91%. The shear span ratio, a/d, is 3. The mesh for concrete uses 3D continuum hexahedral elements of size 12.5 mm, which are kept the same for all sizes in order to avoid dealing with spurious mesh sensitivity due to localization of softening damage. The reinforcement is modeled with 2-node linear beam elements attached at nodes to the elements of concrete. The smallest FE system has 1,457 nodes and 990 elements, while the largest one has 78,895 nodes and 58,347 elements.

Figure 4b shows the verification and calibration results for tests conducted in Ref. 31. Beams of three sizes are tested with a 4-point bending load configuration. The effective depths of beams are 160, 360 and 750 mm. The reinforcement ratio is 1.0% and the aspect ratio, a/d, is 3. The maximum aggregate size is 10 mm. The element size is 20 mm, for all the sizes. 3D continuum elements with reduced integration are used in explicit (dynamic) analysis.

Figure 4c demonstrates the results for Walraven tests[43] for normal weight concrete. Three different sizes with effective depths of 125, 420 and 720 mm with four-point bending configuration are modeled and calculated using 3D hex elements. The concrete strength is 34.2 MPa and the reinforcement ratio slightly varies from 0.75% to 0.83%. Figure 4

also shows the differences in the ultimate shear strength predictions of CSCT for the used tests. The variation of the secondary parameters other than the size could result in very high discrepancies for ultimate strengths between the SEL and CSCT. For example, in Figure 4c, the difference reaches to 29% for small sizes and doubles for $d \to \infty$.

APPENDIX 3. FOR COMPARISON: GENERAL DERIVATION OF SEL FROM ENERGY CONSERVATION AND DIMENSIONAL ANALYSIS

The total release of (complementary) strain energy Π caused by fracture is a function of both (a) the length a_c of the fracture (or crack band) at maximum load, and (b) the area of the zone damaged by fracturing, which is $w_c a_c$, where $w_c = n d_g$ = material constant = width of crack band swept by FPZ width during propagation of the main crack, d_g = maximum aggregate size, and $n = 2$ to 3. Parameters a_c and $w_c a_c$ are not dimensionless, but can appear only as dimensionless parameters, which may be taken as $\beta_1 = a_c/d$ and $\beta_2 = w_c a_c/d^2$, where d = beam depth. According to the Buckingham theorem of dimensional analysis, the total strain energy release must have the general form:

$$\Pi = \frac{1}{2E}\left(\frac{P}{bd}\right)^2 bd^2 f(\beta_1, \beta_2) \tag{C1}$$

where b = characteristic beam width (e.g., b_w). In the case of geometrically similar beams of different sizes, f is a smooth function independent of d. Now consider the first two linear terms of the Taylor series expansion $f(\beta_1, \beta_2) \approx f(0, 0) + f_1\beta_1 + f_2\beta_2$, where $f_1 = \partial f/\partial\beta_1$, $f_2 = \partial f/\partial\beta_2$, and note that

$$\frac{\partial f}{\partial a_c} = \frac{\partial f}{\partial \beta_1}\frac{\partial \beta_1}{\partial a_c} + \frac{\partial f}{\partial \beta_2}\frac{\partial \beta_2}{\partial a_c} \tag{C2}$$

in which $\partial\beta_1/\partial a_c = 1/d$ and $\partial\beta_2/\partial a_c = w_c/d^2$. The energy conservation during crack propagation requires that $[\partial\Pi/\partial a_c]_P = G_f b$, where G_f = critical value of energy release rate. This leads to the equation

$$\left(\frac{f_1}{d} + \frac{f_2 w_c}{d^2}\right)\frac{P^2}{2bE} = G_f b \tag{C3}$$

After rearrangement, and using the notation $v_u = P/bd$ = average (or nominal) shear strength due to concrete, Equation (C3) yields the deterministic (or energetic) size effect of ACI-446 (now embedded in ACI-318-2019), with the size effect factor λ given by Equation (8), in which $d_0 = w_c f_2 / f_1$ = constant (independent of size d, transitional size characterizing structure geometry). Q.E.D.

The hypotheses underpinning this derivation are two: (a) The size, w_c (width or length), of the FPZ at the front of dominant crack is constant (a material property), and (b) the failures are geometrically similar (this similarity is not listed

here among the hypotheses of CSCT but is tacitly implied). Energy conservation is not a hypothesis but a physical fact. Neither is Equation (C1), which is dictated by dimensional analysis. Note that the fracture mechanics had not to be specifically invoked in this derivation, although energy balance is the quintessential basis of fracture mechanics.